

Performance Multicriteria Optimization of Locally Fabricated Hammer Mill using Population Balance Model

B. Kengne^{1*}, M. P. Ndibi Mbozo'o¹, W. Nzie¹, D. Tcheukam-Toko² & Ali Ahmed³

¹Department of Mechanical Engineering, ENSAI, University of Ngaoundere, Cameroon. ²Department of Mechanical Engineering, College of Technology, University of Buea, Cameroon. ³Department of Chemistry Engineering, UIT, University of Ngaoundere, Cameroon. Corresponding Author (B. Kengne) Email: benjaminkengne@gmail.com*



DOI: <https://doi.org/10.38177/ajast.2023.7308>

Copyright: © 2023 B. Kengne et al. This is an open-access article distributed under the terms of the Creative Commons Attribution License, which permits unrestricted use, distribution, and reproduction in any medium, provided the original author and source are credited.

Article Received: 11 June 2023

Article Accepted: 14 August 2023

Article Published: 29 August 2023

ABSTRACT

High energy consumption and better prediction of the particle size distribution of outgoing particles in grinding operations are very important issues for manufacturers, so processes need to be optimized to reduce energy consumption and achieve the desired product quality. The optimum grinding parameters for a locally-produced hammer mill for maize kernels were thus determined, so that the equipment could operate under optimum conditions, with low energy consumption, while guaranteeing the quality of the ground kernels. The population balance model (PBM) was used to model the particle size distributions of the milling products in the hammer mill, by determining the model parameters: the selection function, the milling function and the classification function, with R^2 values greater than 0.97. The parameters determined were recalculated by minimizing the residual error between the experimental and simulated size distributions for better correlation. Two objective functions were determined: 1) to minimize the production of fine particles with sizes below 0.25 mm, and 2) to reduce energy consumption. Using genetic algorithms in Matlab, the resolution of the multicriteria problem yielded optimal grinding conditions at maximum feed rate as follows: rotation speed $N_{opt} = 2750$ tr/mn for a sieve $d_{opti} = 4$ mm, for specific energy consumption of less than 5% and fine particle production of less than 20%.

Keywords: Population Balance Method; Size distribution; Multicriteria problem; Specific energy consumption; Locally fabricated hammer mill.

1. Introduction

Maize (*Zea mays* L.), the "queen of cereals", is the most widely used cereal in the world's diet and also in the manufacture of animal feeds, particularly in sub-Saharan Africa; this makes it the most important cereal in terms of production and consumption ahead of rice and millet in West and Central Africa [1],[2]. It is generally preferred to other cereals because it has a more uniform nutritional value and provides better structure to the food, and above all because of its availability [3],[4].

Around two-thirds of the maize grain produced in Cameroon is used in feed mills for the production of animal feed [2]. As a general rule, the first stage in the production of animal feed from maize grain is grinding, which is carried out thanks to the development of mills and grinders equipped with electric or thermal motors. These mills, which used to be imported, are now, for most of the mills used in Cameroon, locally manufactured [5]. These mills or grinders are generally hammer mills, and are the most widely used for dry grinding of maize due to their simple design, easy operation and low maintenance costs [6],[7],[8]. In these mills, the product to be ground is introduced into the grinding chamber by gravity and exits the cylinder when they are small enough to pass through a screen at the bottom [9]. Although functional and increasing in demand (due to the cost of purchase), this locally-designed equipment does not always meet users' expectations, and does not preserve the organoleptic qualities of the flour obtained.

The process of grinding cereal grains in hammer mills is complex and not fully understood [10]. Currently in particle milling, producing a ground product to the desired size with minimal energy consumption is the most challenging task for a process engineer [11]. It is important to understand the factors that affect performance

parameters such as energy consumption per unit mass and the particle size distribution of the product leaving the mill [12],[13].

Several studies have been carried out to contribute to this scientific challenge. Some studies are mainly focused on investigating the efficiency of the hammer mill in terms of particle size distribution of the output product, energy consumption and yield [7],[14] by adopting an empirical approach that consisted in modeling these performance criteria as a function of a few defined variables.

On the other hand, other studies are limited to investigating the kinetics of particle breakage in a small hammer mill [15],[16] and the strength characteristics of particle under impact fracture [17]. However, studies evaluating the effect of hammer mill parameters on performance criteria are rarely reported in the literature [18],[19]. Note also that semi-empirical energy models by Rittinger, Kick, or Bond, have been widely applied to model the energy consumed during grinding as a function of product size at the mill inlet and outlet, during grinding in hammer mills [14],[20]. Other semi-empirical models used to smooth the particle size distribution curves of the grinding result using simplified laws such as the Gaudin-Schuman, Rosim-Rammler-Bennet or law [21],[22]. However, these approaches are incomplete, and lack appropriate physical understanding.

In order to comprehensively predict the complete particle size distribution for a given set of operating conditions, population balance models have frequently been used. It is most often used to mathematically describe the crushing process [12],[23],[24],[25]. In the following, we present the population balance approach as a tool for mechanistic modeling of grinding in hammer mills.

2. Mathematical Modeling of Hammer Mill

2.1. Population Balance Model (PBM)

In the case of grinding, in addition to their ability to predict the particle size distribution of the process, mechanistic models contribute to the understanding of the physical phenomena involved. They are based on the fundamental laws governing the behavior of the process under study. According to [26], grinding can be considered as a succession of unitary stages, essentially consisting of the selection of a material fraction in the first stage, followed by the grinding of this material fraction in the second stage, to which is added the classification of this material fraction in the case of screen mills.

The general form of the population balance equation for grinding is described as follows [27],[28]:

$$\frac{dm(x,t)}{dt} = [\text{Input}] - [\text{Output}] + [\text{Birth}] - [\text{Disappearance}] \quad (1)$$

In equation (1), $m(x, t)$ represents the mass fraction of particles of size x present in the mill during the time interval dt . Birth and Disappearance respectively represent the increase or decrease in particle mass fraction due to the grinding process. Input represents particles entering the mechanism, and output represents particles leaving the system.

Based on this kinetic approach, [29] proposed equation (2), representing the discrete form of equation (1), to model hammer mills with a built-in sieve [30]:

$$\frac{dm_i(x,t)}{dt} = \dot{m}_{in,i}(x,t) - \dot{m}_{out,i}(x,t) + \sum_{j=1}^{i-1} S_j(x) b_{i,j}(x) m_j(t) - S_i(x) m_i(t) \quad (2)$$

where the output is,

$$\dot{m}_{out,i}(x,t) = C_i(x) m_i(t) \quad (3)$$

In equation (2), $\dot{m}_{out,i}(x,t)$ and $\dot{m}_{in,i}(x,t)$ represents on the time t , the particles outflow and inflow rates in the mill, the particle was size or fraction i . $S_i(x)$ (s^{-1}) is the rate of disappearance of particles of size i that are ground at time t , or selection function. $b_{i,j}(x)$ is the size distribution of particles of size j that have ground to size i at time t , or grinding distribution function. $C_i(x)$ is the rate of the mass fraction of particles of size i leaving the mill, and τ the residence time of the particles inside the mill.

This equation implies that the quantity of material of size i evolves due to three phenomena:

- It decreases as size i decreases, expressed by the selection function $S_i(x)$.
- It increases due to the addition of material of size i , resulting from the grinding of larger particles. The grinding distribution function refers to the material of size j that fragments for size i .
- It also decreases due to particles of size i leaving the mill, reflected by the classification function C_i .

In order to develop a mill model, it is generally assumed that the material passing the screen has remained in the mill for an extremely short time [31].

This model is based on the determination of these three functions. In practice, this means the evolution of the particle size distributions of particles of any size over time. The challenge then is to select an appropriate selection function S_i , milling distribution functions b_{ij} and classification matrix C_i , and to make these choices physically relevant [31]. There has been some progress in basing these functions on material properties and equipment design variables [32],[33], but fracture modeling still remains difficult due to the difficulty of measuring their intrinsic mechanical properties, which are linked not only to the fracture behavior of the material but also to the operating conditions of the equipment.

The vast majority of research work that has focused on modeling grinding with a classification system external to the mill [11],[14],[34]. Reference [35], [36] and other researchers, build on this concept to develop models for simulating and predicting grinding processes. They defined grinding selection and distribution functions, continuous in time and discrete with respect to the size classes of ground particles.

Still on the subject of applications, [10] developed a steady-state population balance model of a laboratory-scale hammer mill to predict the particle size distribution for two biomass resources, which are characterized by non-brittle fibrous behavior and non-spherical particle shape, analyzing the effects of material properties and operating variables. Long before him, [23] explored the modeling of hammer milling of corn, in particular for continuous and regular milling in a laboratory-scale apparatus.

Reference [9] proposed the dynamic modeling of corn kernel grinding in hammer mills using a population equilibrium approach. Corn grinding was tested in pilot and industrial continuous hammer mills, under different operating conditions. The results of the pilot experiments were used to adjust the parameters of the selection and classification functions, taking into account the effects of rotor speed and screen aperture size. The model was validated with steady-state data at both pilot and industrial scale, which also included variations in feed rates.

2.2. Matrix Form for Hammer Mill Modelling

2.2.1. Matrix form of PBM

The equation of the balance approach can be solved numerically in several ways, including using the matrix method [37],[38]. The matrix form of the population balance model for predicting hammer mill performance is inspired by the structure model adapted from [10].

Figure 1 below shows the hammer mill structure model used for the matrix form of the population balance equation. For this case study, the sieve or classification system is incorporated into the mill.

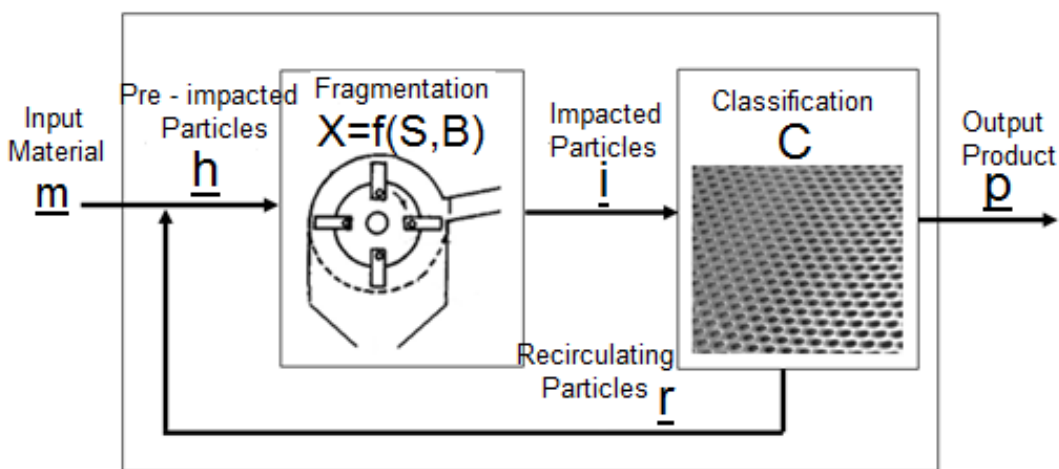


Figure 1. Representation of a hammer mill with an adapted sieve by [10]

In this fig. 1, m is the size distribution of the input material, i the size distribution of the material after impact and before the internal sieve, p is the size distribution of the output product leaving the mill throughout the internal sieve and r the recirculating particles that were unable to pass through the sieve according to their size.

The matrix script adopted for grinding in the hammer mill is therefore:

$$p = C \cdot X \cdot [I - (I - C) \cdot X]^{-1} \cdot m \quad (4)$$

where I is the identity matrix. C is the classification matrix, with is diagonal matrix whose elements represent the classification efficiency for each size interval of material. X is the fragmentation matrix, which summarizes the fundamental mechanisms governing particle breakup in the mill, and particle-particle and particle-screen collisions are considered negligible. It is presented in equation (5) below:

$$X = b \cdot S + I - S \quad (5)$$

where b is a lower triangular matrix that represents the breakage distribution matrix and S is a diagonal matrix which means breakage rate matrix.

These relationships are widely accepted by many authors [10],[38] |[39],[40].

2.2.2. Expression of different function

2.2.2.1. Selection function

The values of the breakage rate function also called selection function S_i describe the grinding rate during the unit of time. It is strongly influenced by grinding conditions (especially rotational speed) and material properties [9],[33]. Its expression is defined by equation (6) [41],[42]:

$$S_i = \lambda_1 N \left(\frac{x_{pi}}{d_{po}} \right)^{\lambda_2} \quad (6)$$

where x_{pi} is the representative particle size in class i. N is the rotational speed of the hammer mill rotor in tr/mn and d_{po} is size reference equal to the maximum corn kernel size. The parameters λ_1 and λ_2 are the parameters of the function to fitted using experimental data.

2.2.2.2. Breakage distribution function

The breakage distribution function b_{ij} describes the new particle population generated from grinding the parent particle. The grinding function is characteristic of the product to be ground. The form for the cumulative breakage distribution function proposed by [43], and intensively used by various authors [6],[9],[14], is defined in equation (7) :

$$B_{ij} = \begin{cases} \varphi \left(\frac{x_{pi-1}}{x_{pj}} \right)^\gamma + (1 - \varphi) \left(\frac{x_{pi-1}}{x_{pj}} \right)^\beta & i > j \\ 1 & i \leq j \end{cases} \quad (7)$$

And the breakage distribution function obtains from the cumulative function is:

$$b_{ij} = B_{ij} - B_{i+1j} \quad (8)$$

where x_{pi-1} is the representative particle size on the class i-1, x_{pj} is the representative particle size of input material on the class j ; φ , γ et β are the parameters characterizing the breakage distribution function or its cumulative form that must be adjusted on the basis of experimental data.

2.2.2.3. Classification function

When the particles undergo grinding, they fall onto the sieve, where they are either retained to be ground into fine particles, or leave the grinding chamber, depending on their size. The population balance approach defines a probability function called the classification function, which translates this step.

Following [31], [44] proposes a classification function (defined by the C_i matrix) defined by equation (9) below:

$$C_i = 1 - \left(\frac{x_{pi}}{\mu d_s} \right)^{\alpha_1} \quad (9)$$

with

$$\mu = f(N, d_s) = \alpha_2 + \alpha_3 N + \alpha_4 d_s$$

where d_s is the size of the sieve mesh, μ is the critical size factor that takes into account the rotational speed of the hammer mill rotor and the size of the sieve mesh, α_1 is the adjustment parameter that determines the sensitivity of particle size on the efficiency of the classification function. $\mu \cdot d_s$ is the maximum particle size that can exit the mill. As particle size approaches this maximum size of particles that can exit the mill, the probability of classification becomes zero, i.e if $x_{pi} > \mu \cdot d_s$, then $C_i = 0$ (particles are held back to undergo possible fragmentation).

Two methods exist for determining S_i , b_{ij} and C_i . The most widely used, which uses both direct measurement and back-calculation from experimental grinding data [45],[46],[47]. And the other so-called "direct measurement" method requires tedious breaking experiments on many one-dimensional feeds to determine the parameters without resorting to complex non-linear optimization methods.

Particle size distribution is one of the main sources of information for milling, as it has a considerable influence on other processes after milling. One of the aspects to be taken into account when modeling flour particle size distribution is the variation in the production of fine particles (sizes below 0.25 mm). The greater or lesser presence of these particles is a source of multiple problems, including explosion risks, health hazards and product loss in the form of emitted dust [48]. Yet local SME workers are more exposed to these risks due to the use of ageing equipment, an inadequate working environment, a lack of awareness of the health risks due to exposure to airborne particles [49],[50].

Thus, process optimization, based on accurate prediction of particle size distribution at the mill outlet, should aim to reduce the rate of fine particle production and cut energy consumption by avoiding over-grinding. And today's requirements for the manufacture of processing equipment make it essential to develop research into cereal milling, with a view to ensuring food quality that meets the physiological needs of consumers. The most important research activity in cereal milling is therefore to obtain a final product with a uniform granulometric composition, a desired particle size and minimal energy costs. The aim of our work is therefore to:

- model the particle size distribution of corn flours obtained from a locally manufactured mill;
- determine the operating conditions that will reduce the quantity of fine particles produced, while consuming less energy during grinding.

3. Materials and Methods

3.1. Material

3.1.1. Locally fabricated hammer mill

A pilot hammer mill is manufactured in a workshop in Ngaoundere by a local manufacturer. It is fitted with a rotor carrying 16 hammers and a sieve. The diameter of the hammer tip is 470 mm and the width of the crusher is 70 mm. The hammers are rectangular, 43 mm wide and 150 mm long. The specifications of the hammer mill used for the experiment are listed in Table 1.

Table 1. Features of the locally manufactured hammer mill

| | | |
|---------------------------------------|------------------------|-------------------------|
| Fabrication | | Locally manufactured |
| Capacity | | 1000 kg/h |
| Hammer | Number per line | 4 |
| | Line | 4 |
| | Shape | Plate |
| | Dimensions (mm) | 4 x 50 x 120 |
| | Weight (kg) | 250 g |
| Sieve | mesh (mm) | 2 mm et 8 mm |
| Energy | Origin | Electrical |
| | Power | 7.5 kW |
| | Transmission | Pulleys - belt |
| | Motor speed | 3000 tr/mn |
| Grinding chamber | Design | Circular |
| | Width (mm) | 250 mm |
| | Inner diameter | 600 mm |
| Space between hammer and sieve | | Between 3 to 4 mm |
| Diameter of the rotor (mm) | | 390 hammer edge to edge |

3.1.2. Measurement and laboratory equipment

a K-tronic vibrating sieve shaker equipped with 6 sieves with mesh sizes of 0.25 mm, 0.425 mm, 0.60 mm, 0.85 mm, 1.00 mm and 1.6 mm respectively, plus a collection bottom. This will enable particle size analysis of the flour fractions obtained from grinding corn kernels. A high precision digital balance was used to weigh the maize kernels and for particle size analysis. And we use a wattmeter for measuring the power consuming by the hammer.

3.1.3. Crops material

White maize, composite variety 'Shaba' (see in fig. 2.) was selected with a moisture content of $13 \pm 1\%$. Impurities such as plastic strips, stones, maize straw and metal were removed from the maize batch by sieving through a 6.3 mm wire mesh combined with natural airflow ventilation, and also removed manually.



Figure 2. White maize, composite variety “Shaba”

The maize kernels are collected on the local market. Maize kernels of this variety are generally between 6 mm and 12 mm in size [51]. Using 6 mm and 10 mm sieves, maize kernels are grouped into three classes, as shown in the table below:

Table 2. Different size classes of maize kernels

| Classes | I | II | III |
|-----------|----------|----------|---------|
| size (mm) | < 6.3 mm | [6.3–10] | ≥ 10 mm |

3.2. Method

3.2.1. Experimental procedure

To develop a model for predicting product size distribution in locally manufactured hammer mills, three categories of experiments (experiments A, B and C) were carried out.

- Experiment A: a mass $m = 4$ kg of corn grain of each class is introduced into the mill, with the outlet blocked by an unperforated metal plate, for 5 minutes. The variables defined for this experiment are feed rate (Partially Open and Totally Open) and rotor speed (2000 and 3000 rpm).
- Experiment B: operating conditions are the same as for experiment A, but the metal plate is removed and replaced by sieves with aperture sizes of 2 mm, 5 mm and 8 mm.

These two experiments will be used to determine the parameters of the selection, grinding and classification matrices.

- Experiment C: Corn kernels are fed into the grinder without taking into account the different classes. The aim of this experiment is to validate the performance model defined by matrices S, B and C. the composition of the samples used in this experiment according to grain size is given in the table 3 below:

Table 3. Composition of the samples

| Kernel size | < 6.3 mm | [6.3 – 10] | > 10 mm |
|---------------------|----------|------------|---------|
| Mass fraction (%) | 0.22 | 0.51 | 0.27 |
| Xpi (mm) | 4.35 | 7.94 | 11.18 |
| d ₁ (mm) | 8.025 | | |

In this experiment, we measured the power consumed. And using (equation 10), we calculated the specific energy consumption by the hammer mill.

$$E_{spec} = \frac{\Delta P \times t}{M} \quad (10)$$

In (equation 10), P is the difference between the power consumed at no load and the load power consumed, t is the time during the grinding has done and M is the grinding maize kernel.

In terms of operational parameters, three variables are considered:

- The size of the sieve in the mill (ds), which impacts the product size distribution. Three mesh sizes were chosen: 2 mm, 5 mm and 8 mm.
- Rotor speed (N), which affects impact energy: 2000 tr/mn, 2500 tr/mn and 3000 tr/mn.
- Mill feed rate, which influences grain-to-grain interaction inside the grinding chamber. Depending on the habits of local operators, two feed rates are chosen, in relation with size of opening hopper feeding: either totally open (TO) or partially open (PO).

All the combinations of these variables give us a total of 20 tests for experiment A, 30 tests for experiment B and 18 tests for experiment C.

Particle size analysis is performed by sieving 100 g of ground product using a K-tronic sieve shaker with six sieves of respective sizes of 1.6 mm, 1 mm, 0.8 mm, 0.63 mm, 0.45 mm, 0.25 mm and pan.

3.2.2. Experimental values of S and B matrix

Experimental values of **S** and **B** are determined using the relationships below.

S values are assumed to be independent of time [52]. The values of the **Si** matrix are calculated by (equation 11):

$$\log \left[\frac{m_{nbi}}{m_{oi}} \right] = - \frac{S_i \times t}{2,3} \quad (11)$$

where **m_{nbi}** is the mass of unground material (g) in class i, **m₀** is the initial mass of maize introduced into the mill and t is the the estimated grinding time for the mass of 4000 gr.

For values of **b_{ij}**, corresponding to the fraction of mass of size j that appears in size interval i after primary grinding, is determined using (equation 8) defined above. **B_{ij}** values are determined experimentally from the particle size

analysis of the product of short-term grinding of a single starting mass of size j (BII method) described by [45], using (equation 12):

$$B_{i,j} = \frac{\ln \left[\frac{1 - P_i(0)}{1 - P_i(t)} \right]}{\ln \left[\frac{1 - P_{j+1}(0)}{1 - P_{j+1}(t)} \right]} \quad (12)$$

$P_i(t)$ is the weight fraction below the top size of size range i after grinding time t .

3.2.3. Back calculation parameters

The values of the optimized parameters of the C , S and B matrix are determined using the back-calculation procedure described in Fig. 3 below. Back-calculation, a technique which involves calculating the model parameters that best fit the experimental data, is also widely used and offers significant advantages over direct measurements [34],[47],[53]. Linear and non-linear optimization techniques are usually combined, or combined with other approximate solutions, to recalculate the model parameters [54],[55].

Figure 3 shows a diagram of the procedure for retro-calculating the parameters of the selection, grinding and classification functions.

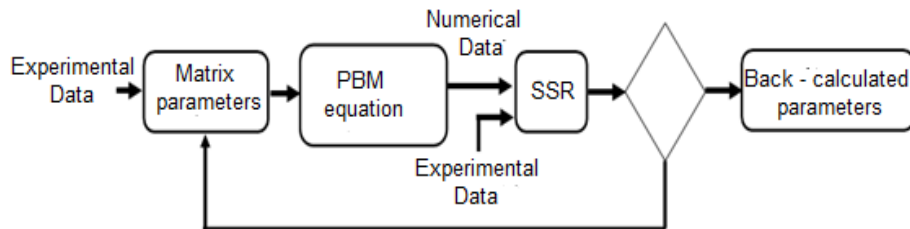


Figure 3. Schematic diagram of the back – calculation procedure adapted from [24]

The optimal values of the fitted parameters are estimated by minimizing the objective function (sum of squares of the residuals), defined by (equation 13) below:

$$\text{Min } SSR = \sum_{i=1}^n (Y_{\text{exp},i} - Y_{\text{sim},i})^2 \quad (13)$$

The optimization method to back-calculate these parameters of matrix S , B and C was carried out using the "fmincon" nonlinear optimizer in MatLabTM 2019. "fmincon" uses the "point-interior" algorithm to solve the nonlinear optimization problem in question, and is suitable for general nonlinear optimization [47],[56].

3.2.4. Specific energy consumption modelling

For our study and based on the work of [5],[21],[59], we hypothesize that the specific energy consumed E_{spec} by the local fabricated hammer mill is modeled by the Rittinger energy law, whose expression is described by the equation (14):

$$E_{\text{spec}} = K \left(\frac{1}{d_2} - \frac{1}{d_1} \right) \quad (14)$$

with d_1 and d_2 are the feed and product size, respectively; and K is a Rittinger constant. In this equation (14), the product size d_2 is calculated by the equation (15):

$$d_2 = \sum_{i=1}^n X_{pi} \square p_i \quad (15)$$

where p_i is the mass fraction of product retained of sieve of size d_{pi} , during the particle size analysis, and X_{pi} is the geometric mean diameter of particles of i^{th} sieve, assumed to be described by the equation (16) below:

$$X_{pi} = \sqrt{D_{p,i} \square D_{p,i-1}} \quad (16)$$

where $d_{p,i}$ and $d_{p,i+1}$ the diameter of sieve openings respectively of the i^{th} sieve and $(i+1)^{\text{th}}$ sieve.

The value of the constant K is determined by adjusting the values of specific energy consumed obtained experimentally with those simulated using the relationship (14) of the rittinger's energetic law.

3.2.5. Determining optimum operating conditions

In our study, we wish to have only particles whose size is greater than 0.25 mm; the standard stipulates that less than 25% of the flour must pass through a sieve with a mesh size of 0.25 mm [57] so our study aims to minimize particles with sizes smaller than 0.25 mm when grinding cereal corn in a locally manufactured hammer mill.

In the case of a multi-criteria problem, the challenge is to determine a solution that is an acceptable compromise between all the criteria considered. In the case of grinding, we have defined two optimization criteria: the specific energy consumed and the quality of the ground product. Cereal grinding using a hammer mill generates large quantities of fine particles (less than 0.25 mm in size), which are harmful to the environment and the surrounding population. The quantity of fine particles generated depends on several parameters, including rotation speed, feed rate, sieve size and the characteristics of the material to be ground. Our study will focus solely on the "sieve size" variable, as its impact on specific energy and flour quality (particle size distribution and geometric mean size) has been shown to be predominant [9],[58].

Then, the functions to be optimized are as follows:

$$\left\{ \begin{array}{l} \min p_k = p_{n-1} + p_n = 1 - \sum_{i=1}^{n-2} p_i \end{array} \right. \quad (17)$$

$$\left. \min E_{\text{spec}} = K_r \left(\frac{1}{d_2} - \frac{1}{d_1} \right) \right. \quad (18)$$

The particle size distribution of outlet p is described by (equation 4) previous with the fragmentation matrix X described in (equation 5) previous.

with constraints:

$$\left\{ \begin{array}{l} p_i > 0, \quad \forall i \in \{1, 2, 3, \dots, n\} \end{array} \right. \quad (19)$$

$$\left\{ \begin{array}{l} \sum_{i=1}^n p_i = 1 \end{array} \right. \quad (20)$$

$$\left\{ \begin{array}{l} p_k = p_{n-1} + p_n < 0,2 \end{array} \right. \quad (21)$$

The optimization was performed using the "gamultiobj" algorithm, a version of Matlab's NSGA-II. The variables to be optimized in our problem are the speed of rotation and the size of the sieve inserted in the mill. We note $[X_{opt}]$ the optimal values of our parameters.

4. Results and Discussion

4.1. Experimental values of matrix S and B

The experimental values of the S_i selection matrix corresponding to maize particle sizes for different classes are shown in fig. 4.

This shows the influence of the rotation speed on the milling frequency of maize grains. The selection function S increases with the rotation speed of the rotor. We also notice that when the feed rate is growth, the values of S_i increase too. This suggest that a higher fragmentation of the particles needs a higher rotation speed with an important feed rate at the entrance. The theory of the particles rupture shows that the bigger particles break more easily because they contain microcracking more important than the smaller ones [60].

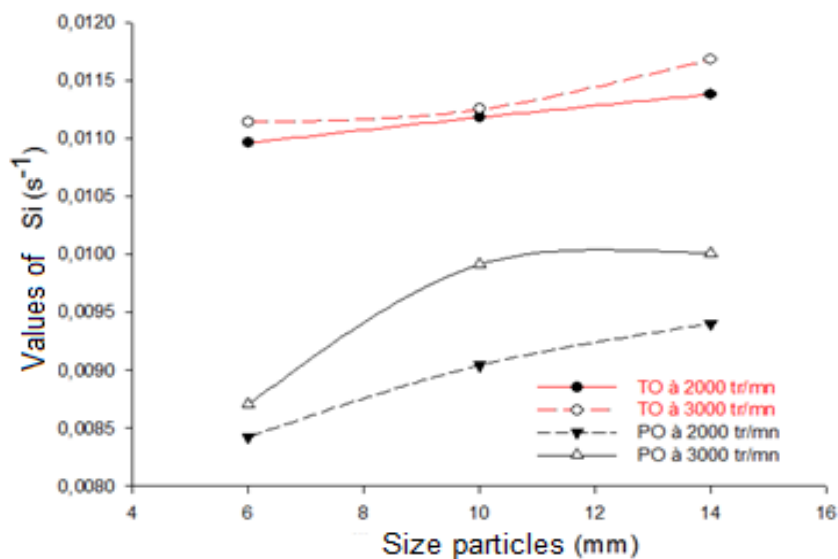


Figure 4. Influence of the feed rate and the rotation speed on the experimental values of S_i

The values of matrix S parameter obtained using experimental data is presented in table 4 below:

Table 4. Parameters values of function S

| Opening hopper | Parameter | λ_1 | λ_2 |
|----------------|-----------|-------------|-------------|
| PO | Value | 3.16 | 2.375 |
| | Sdt error | 0.068 | 0.0529 |
| TO | Value | 3.241 | 2.304 |
| | Sdt error | 0.056 | 0.0540 |

Experimental values for the grinding matrix are calculated using the BII method (equation 12), which is used for a very short grinding time based on data obtained in experiment A. The results obtained are presented in Tables 5 and 6 for the partially open and fully open hopper experiments.

Table 5. Experimental values of $B_{i,j}$ and $b_{i,j}$ at PO hooper

| Class of particles sizes | | $V = 2000 \text{ tr/mn}$ | | | | | | $V = 3000 \text{ tr/mn}$ | | | | | |
|--------------------------|-----------|--------------------------|-----------|-----------|-----------|------------|-----------|--------------------------|-----------|-----------|-----------|------------|-----------|
| | | <i>I</i> | | <i>II</i> | | <i>III</i> | | <i>I</i> | | <i>II</i> | | <i>III</i> | |
| | | $B_{i,1}$ | $b_{i,1}$ | $B_{i,2}$ | $b_{i,2}$ | $B_{i,3}$ | $b_{i,3}$ | $B_{i,1}$ | $b_{i,1}$ | $B_{i,2}$ | $b_{i,2}$ | $B_{i,3}$ | $b_{i,3}$ |
| i = | 1 | 1 | 0 | | | | | 1 | 0 | | | | |
| | 2 | 1 | 0.216 | 1 | 0 | | | 1 | 0.159 | 1 | 0 | | |
| | 3 | 0.784 | 0.239 | 1 | 0.357 | 1 | 0 | 0.841 | 0.217 | 1 | 0.247 | 1 | 0 |
| | 4 | 0.545 | 0.082 | 0.643 | 0.156 | 1 | 0.451 | 0.624 | 0.107 | 0.753 | 0.158 | 1 | 0.366 |
| | 5 | 0.463 | 0.211 | 0.487 | 0.18 | 0.549 | 0.178 | 0.517 | 0.144 | 0.595 | 0.21 | 0.634 | 0.196 |
| | 6 | 0.252 | 0.058 | 0.307 | 0.061 | 0.371 | 0.098 | 0.373 | 0.116 | 0.385 | 0.193 | 0.438 | 0.151 |
| | 7 | 0.194 | 0.112 | 0.246 | 0.154 | 0.273 | 0.127 | 0.257 | 0.114 | 0.192 | 0.09 | 0.287 | 0.142 |
| | 8 | 0.082 | 0.056 | 0.092 | 0.058 | 0.146 | 0.091 | 0.143 | 0.046 | 0.102 | 0.018 | 0.145 | 0.05 |
| | 9 | 0.026 | 0.017 | 0.034 | 0.018 | 0.055 | 0.034 | 0.097 | 0.082 | 0.084 | 0.048 | 0.095 | 0.05 |
| | 10 | 0.009 | 0.009 | 0.016 | 0.016 | 0.021 | 0.021 | 0.015 | 0.015 | 0.036 | 0.036 | 0.045 | 0.045 |

The grinding matrix represents the cumulative size distribution of the child particle fractions resulting from the primary grinding of the mother particle.

Table 6. Experimental values of $b_{i,j}$ and $B_{i,j}$ at TO hooper

| Classes of particles sizes | | $V = 2000 \text{ tr/mn}$ | | | | | | $V = 3000 \text{ tr/mn}$ | | | | | |
|----------------------------|----------|--------------------------|-----------|-----------|-----------|------------|-----------|--------------------------|-----------|-----------|-----------|------------|-----------|
| | | <i>I</i> | | <i>II</i> | | <i>III</i> | | <i>I</i> | | <i>II</i> | | <i>III</i> | |
| | | $B_{i,1}$ | $b_{i,1}$ | $B_{i,2}$ | $b_{i,2}$ | $B_{i,3}$ | $b_{i,3}$ | $B_{i,1}$ | $b_{i,1}$ | $B_{i,2}$ | $b_{i,2}$ | $B_{i,3}$ | $b_{i,3}$ |
| i = | 1 | 1.000 | 0.000 | | | | | 1.000 | 0.000 | | | | |
| | 2 | 1.000 | 0.205 | 1.000 | 0.000 | | | 1.000 | 0.109 | 1.000 | 0.000 | | |
| | 3 | 0.795 | 0.233 | 1.000 | 0.160 | 1.000 | 0.000 | 0.891 | 0.207 | 1.000 | 0.247 | 1.000 | 0.000 |
| | 4 | 0.562 | 0.278 | 0.840 | 0.190 | 1.000 | 0.170 | 0.684 | 0.397 | 0.753 | 0.244 | 1.000 | 0.284 |

| | | | | | | | | | | | | | |
|--|-----------|-------|-------|-------|-------|-------|-------|-------|-------|-------|-------|-------|-------|
| | 5 | 0.284 | 0.111 | 0.650 | 0.274 | 0.830 | 0.176 | 0.287 | 0.114 | 0.510 | 0.202 | 0.716 | 0.179 |
| | 6 | 0.173 | 0.088 | 0.376 | 0.225 | 0.654 | 0.256 | 0.173 | 0.088 | 0.308 | 0.139 | 0.538 | 0.297 |
| | 7 | 0.085 | 0.032 | 0.151 | 0.055 | 0.398 | 0.227 | 0.086 | 0.032 | 0.169 | 0.086 | 0.241 | 0.135 |
| | 8 | 0.053 | 0.022 | 0.096 | 0.044 | 0.171 | 0.097 | 0.054 | 0.009 | 0.083 | 0.040 | 0.106 | 0.005 |
| | 9 | 0.031 | 0.016 | 0.052 | 0.031 | 0.074 | 0.041 | 0.045 | 0.029 | 0.057 | 0.031 | 0.101 | 0.017 |
| | 10 | 0.015 | 0.015 | 0.021 | 0.021 | 0.033 | 0.033 | 0.016 | 0.016 | 0.026 | 0.026 | 0.084 | 0.084 |

The values of $B_{i,j}$ as a function of particle size obtained from BII calculations for the parent fraction > 10 mm in size are shown in Fig. 5 above.

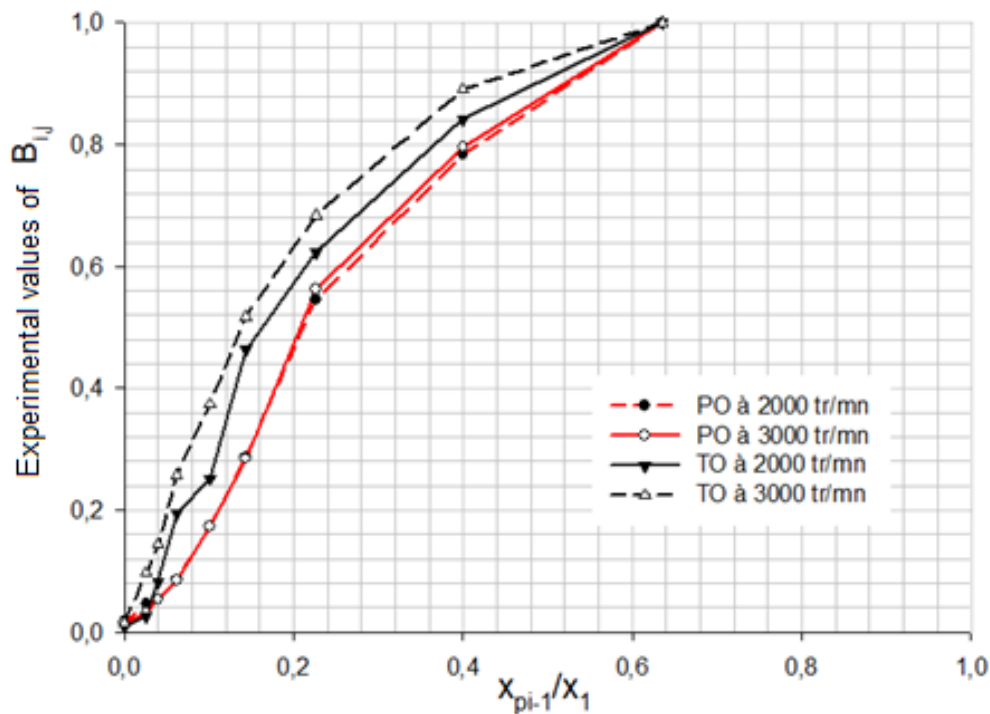


Figure 5. Experimental values of $B_{i,1}$ for maize size fraction > 10 mm

The following observations can be made from Fig. 5 above, when compared with the results obtained from other maize grain fractions:

- The feed rate and rotation speed slightly improve the size distribution of the ground product; finer particle sizes are observed when the hammer mill is sufficiently fed and rotates faster, showing that these two conditions favor a greater quantity of grain being subjected to fractionation; and the rotation speed being high, the fractionation energy is considerable, resulting in smaller particle sizes.
- The results obtained show that changes in mill operating conditions do not lead to significant changes in the values of the parameters ϕ and γ . This observation is in agreement with previous studies [61],[62] which also indicate that the parameters $b_{i,j}$ are independent of mill operating conditions.

These plots show that the grinding function does not depend on the initial particle size, so the grinding distribution function can be considered normalizable. In this way, the values of B can be fitted to the empirical relationship, and the parameters of the grinding function are determined and presented in Table 7 below:

Table 7. Parameters values of function B

| Opening hopper | Parameters | ϕ | β | γ |
|----------------|------------|--------|---------|----------|
| PO | Value | 0.328 | 3.102 | 0.809 |
| | Sdt error | 0.004 | 0.0141 | 0.008 |
| TO | Value | 0.331 | 3.275 | 0.812 |
| | Sdt error | 0.004 | 0.0129 | 0.007 |

4.2. Result of experiment B and estimated parameter values of the classification function

The same experiments were then carried out, but the sieve was left open. The values obtained after particle size analysis of the flours obtained are given in the table below. The cumulative mass fractions obtained from experiment **B** are presented in Table 8 below for grain sizes ranging from 6.3 to 10 mm.

Table 8. Cumulated fractions obtained during experience B for the partially opened hopper

| Sieve (mm) | V= 2000 tr/mn | | | V= 2000 tr/mn | | | V= 3000 tr/mn | | | V= 3000 tr/mn | | |
|---------------|---------------|-------|-------|---------------|-------|-------|---------------|-------|-------|---------------|-------|-------|
| | ds = 2 mm | | | ds = 8 mm | | | ds = 2 mm | | | ds = 8 mm | | |
| | I | II | III |
| 1.6 | 100 | 100 | 100 | 100 | 100 | 100 | 100 | 100 | 100 | 100 | 100 | 100 |
| 1 | 99.52 | 98.92 | 99.6 | 95.57 | 96.37 | 95.75 | 99.31 | 100 | 99.97 | 97.89 | 96.37 | 97 |
| 0.8 | 82.17 | 83.31 | 84.39 | 69.85 | 71.98 | 72.17 | 85.08 | 85.77 | 85.99 | 87.54 | 85.83 | 87.22 |
| 0.63 | 58.05 | 59.8 | 62.25 | 47.59 | 48.19 | 49.09 | 61.96 | 62.45 | 61.93 | 62.09 | 60.62 | 62.16 |
| 0.4 | 28.6 | 30.42 | 31.68 | 28.57 | 29.51 | 28.41 | 29.84 | 30.11 | 29.28 | 33.64 | 32.05 | 33.08 |
| 0.25 | 12.97 | 13.87 | 14.55 | 11.92 | 12.47 | 11.83 | 13.3 | 13.47 | 13.23 | 16.52 | 15.81 | 16.48 |
| pan | 3.23 | 4.69 | 4.81 | 1.35 | 1.38 | 1.42 | 3.05 | 2.98 | 2.84 | 2.05 | 1.99 | 2.24 |

This table 8 shows the influence of rotation speed and initial particle size on the particle size distribution at the outlet: for a rotation speed of 2000 tr/mn, the d_{50} (the mean or average particle size of particles) of the products is less than 0.63 mm when using a 2 mm sieve it also mean that 50% of the particles are smaller than 0.63 mm, but is greater when using an 8 mm sieve. At speeds of 3000 tr/mn, the d_{50} is less than 0.63 mm. This shows that as hammer speeds increase, the average geometric size of the final products decreases.

From the results obtained below and using the formulas defined in (equation 9) and (equation 10), we obtain the parameter values shown in Table 9.

Table 9. Parameters values of the classification matrix

| | Parameters | α_1 | α_2 | α_3 | α_4 |
|--------------|------------|------------|------------|------------|------------|
| Hopper PO | Value | 1.097 | 0.844 | 2.133 | 1.243 |
| | Std dev. | 0.088 | 0.0704 | 0.0618 | 0.0413 |
| Hopper TO | Value | 1.123 | 0.873 | 2.152 | 1.370 |
| | Std dev. | 0.092 | 0.0711 | 0.0631 | 0.0441 |

4.3. Matrix parameters values after back - calculation

The parameters of the model ($\lambda_1, \lambda_2, \varphi, \beta, \alpha_1, \alpha_2, \alpha_3$ and α_4) vary as a function of the process variables. Therefore, the idea here, is to find a single set of parameters describing all the experimental data consisted in performing different preliminary estimations and to correlate their parameter values obtained to the process conditions. To increase accuracy, the initial parameters of the selection, breakage distributions and classification functions were initially fixed turn-by-turn to reduce the time of the back-calculation.

Table 10. Optimized function parameter values

| Opening hopper | Parameter | λ_1 | λ_2 | φ | β | γ | α_1 | α_2 | α_3 | α_4 |
|-------------------|-----------|-------------|-------------|-----------|---------|----------|------------|------------|------------|------------|
| PO | Value | 3.05 | 2.30 | 0.330 | 3.28 | 0.811 | 1.095 | 0.866 | 2.141 | 1.31 |
| | Std dev | 0.061 | 0.055 | 0.004 | 0.012 | 0.008 | 0.089 | 0.065 | 0.062 | 0.047 |
| TO | Value | 3.12 | 2.28 | 0.330 | 3.35 | 0.811 | 1.105 | 0.859 | 2.146 | 1.42 |
| | Std dev | 0.064 | 0.057 | 0.004 | 0.014 | 0.008 | 0.083 | 0.070 | 0.062 | 0.046 |

Table 10 summarizes the best combination of back-calculated parameters obtained after simulation with data from Experiment C.

Fig. 6 shows the model's predictive behavior for corn grinding for trials 1, 2, 3 and 5. It compares the experimental size distributions obtained in Experiment C with the simulated distributions for the identified operating cases. In this figure, we observe very good agreement between experimental and predicted values, within the limits of experimental error, as confirmed by the value of the coefficient of determination R^2 .

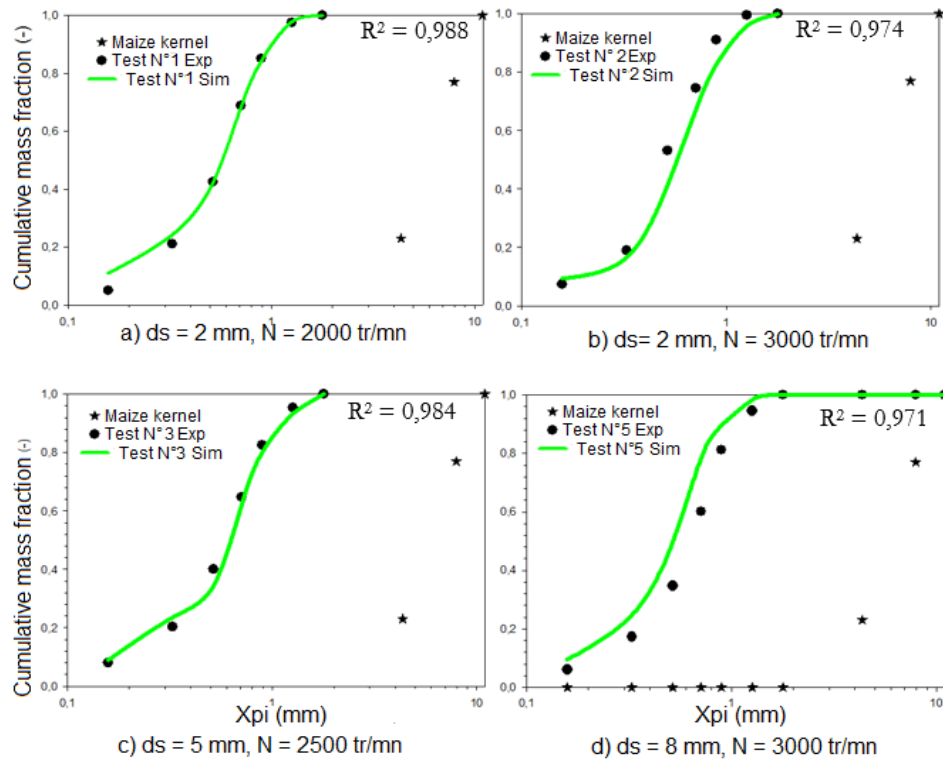


Figure 6. Comparison between experimental and simulated size distribution for partially opened feed hopper (PO)

Overall, Fig. 6 shows a good correlation between the model and experimental data. However, there is a slight lack of precision in the case of higher rotational speed and larger sieve aperture size. In the most favorable cases, the quality of the prediction is visually excellent, to the extent that the prediction error is of the same order of magnitude as the experimental measurement errors.

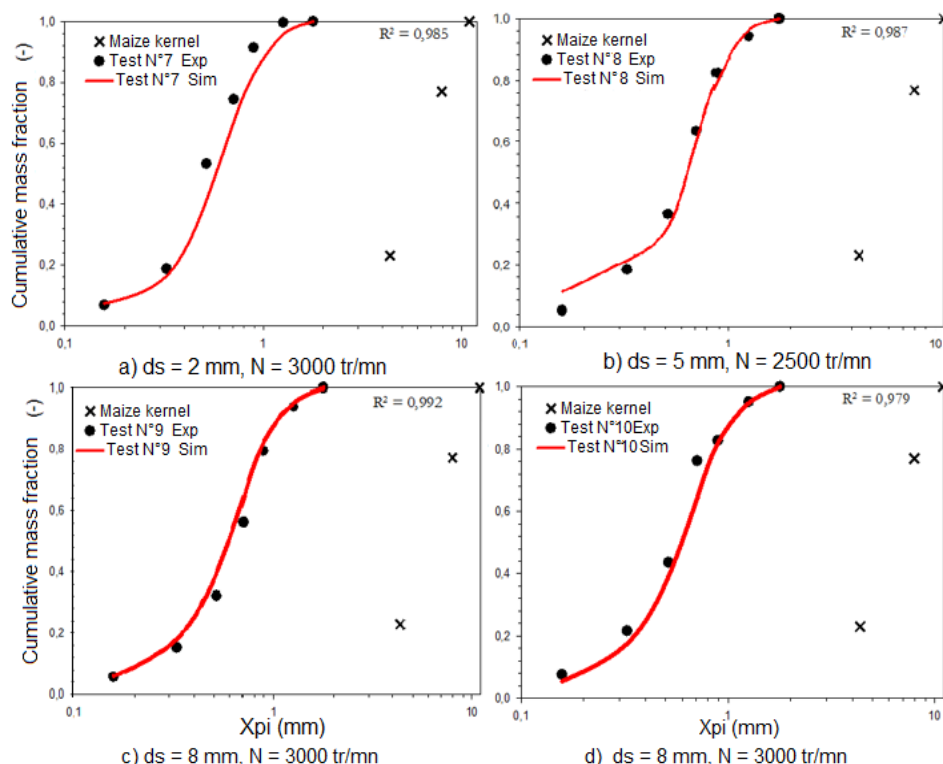


Figure 7. Comparison of experimental and simulated size distribution for a partially open feed hopper (PO)

Experimental and simulated particle size distributions for trials 7, 8, 9 and 10, corresponding to higher mill feed rates (hopper is fully open), are shown in Fig. 7, together with the coefficient of determination (R^2).

These graphs show strong agreement with the experimental data, particularly for test 9 performed at a rotational speed of 2000 rpm with a sieve opening size of 8 mm; and for test 8 performed at a rotational speed of 2500 rpm with a sieve opening size of 5 mm.

For trial 10 (3000 rpm with 8 mm sieve opening size), the correspondence is weaker, although these are the variable parameters for which less experimental data were available; this observation was also made when the mill feed rate was lower, although these were the variable parameters for which less experimental data were available ; this observation was also made when the mill feed rate was lower, suggesting that the model would not fit when for a very high machine feed rate a large screen with a higher rotor speed is used. In general, however, as shown in Fig. 7, the model is able to correctly predict changes in sieve opening size, as well as changes in rotational speed.

From this study, it can be noted that the grinding matrix was independent of rotor speed, mill feed rate and sieve size, but was dependent on grain characteristics. The selection and classification of the material inside the mill depended on the physical configuration and operating characteristics of the mill, as well as on the size of the input particles.

To improve the predictive quality of our model, the following observations are made:

- It seems very important to feed the model with an appropriate set of data for its calibration; this can be achieved by increasing the number of experimental points.
- It is also likely that the nature of the material affects the quality of the prediction. The model specifically models the grinding of maize kernels of a particular variety with a fixed moisture content; characterization errors may therefore be found to be caused by the relative humidity of the working environment, which creates or simulates agglomerations of fine particles.

Despite the good correlation between experimental and simulated observations or data, it is possible that a more mechanistic model could improve the applicability of the study [9],[63]. However, it should be noted that particle crushing or fragmentation is the result of a number of microphenomena that are not very well understood. Complex interactions between particles, particle stress conditions and the environment will determine the outcome of these industrial processes.

4.4. Optimum operating conditions for a locally manufactured hammer mill

For a better presentation of the optimization problem, we assume that the particle size distribution of the output product as a function of the input product is defined by equation (22). Equation (22) is deducted from (4).

$$p = [G] \underline{m} \quad (22)$$

where G is a lower triangular matrix, whose elements is defined in equation (23):

$$\left[G_{ij} \right]_{\substack{0 < i < \\ i \geq i}} = f(N, ds) \quad (23)$$

So our multicriteria optimization problem can be written in the form described in equation (24) below:

$$\left\{ \begin{array}{l} \max \left(2 - \sum_{i=1}^{n-1} G_{n-1,i}(N, ds) \square m_i - \sum_{i=1}^n G_{n,i}(N, ds) \square m_i \right) \\ \min K_r \left(\frac{1}{\sum_{j=1}^n dpi(\sum_{i=1}^j G_{ji} \square m_i)} - \frac{1}{d_1} \right) \end{array} \right. \quad (24)$$

Table 11 below shows the results obtained on Matlab using the "gamultiobj" multi-objective optimization algorithm.

Table 11. Optimum solutions for [Xopt] values in the TO hopper

| Parameters | N | | ds | |
|------------|--------|-------------|------|--|
| | Values | 2750 tr/min | 4 mm | |
| Std dev | 25 | 0.97 | | |

From the values obtained in Table 11, we simulated the particle size distribution of the product and calculated the specific energy consumed. The results are shown in Table 12 below:

Table 12. Simulated flour mass fractions and specific energy consumption for optimum mill operating conditions

| | Espec (KWh/t) | Size of Sieve (mm) | | | | | | | d_{50} (mm) |
|--------|------------------|--------------------|------|------|------|-------|------|------|---------------|
| | | 1.6 | 1.00 | 0.8 | 0.63 | 0.425 | 0.25 | pan | |
| [Xopt] | 4.48 | 0.12 | 0.13 | 0.15 | 0.19 | 0.23 | 0.13 | 0.04 | 763.06 |

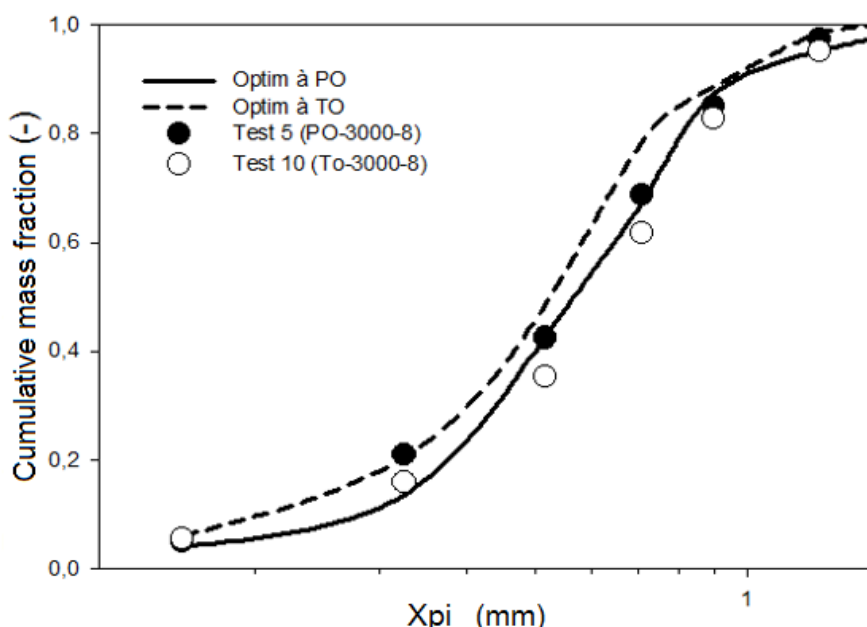


Figure 8. Simulated particle size distributions for [Xopt] compared with tests 5 and 10

Calculating the mass fraction of the last two analysis sieves and comparing with those obtained from experiment C, we note a 20% reduction in fine particles, and 5% lower energy consumption.

Calculating the mass fraction of the last two analysis sieves and comparing with those obtained from experiment C, we note a 20% reduction in fine particles, and 5% lower energy consumption.

Fig.8 above shows the simulated particle size distribution for the optimum operating conditions, which significantly reduce fine particle production with low energy consumption. It can be seen that, in the case of our mill, it would be preferable to operate the mill at a higher feed rate, as this would help to reduce the production of fine particles, but with a sieve with aperture sizes close to 4 mm.

Although there is a difference between partially open and fully open hopper feeding, this difference is not significant in terms of values.

5. Conclusion

Typically, approaches to milling optimization have focused more on improving milling efficiency in terms of quantity produced and energy consumed, thus aiming for higher quantity produced and lower energy consumption during the process. This left very little room for the use of modelling to reduce the quantity of fine particles which are generally lost during transport of the flour produced and also constitute a health risk for the operators of this equipment. The aim of this work is therefore to use milling modeling to optimize flour size distribution, so that the quantity of fine particles produced during milling is reduced or minimized, without increasing the system's energy consumption. To this end, the population balance approach was used to model the particle size distribution of the flour produced; the model obtained proved satisfactory for predicting the particle size distribution of the products leaving our locally-produced hammer mill.

In this study, we have shown that the selection function for particle fracture and the classification function are closely related to rotation speed and sieve size. Both depend on the speed at which particles are available for impact fracture or to pass through the sieve aperture size. As rotational speed increases, more particles can be selected for fracture and pass through the sieve, reducing mass retention. Overall, a model representing the grinding operation in hammer mills has been developed and validated on the basis of steady-state experimental data from mills of different scales. These results are of great value, as they indicate that it is possible to use the fitted model to confidently predict new operating points.

Next, we studied the operation of our mill by defining the optimum operating points of our mill; it emerged that the optimum rotational speed $N_{opti} = 2750$ rpm combined with a sieve size $d_{s,opti} = 4$ mm, contribute to producing fewer fine particles with low energy consumption.

Looking ahead, we can carry out further tests to validate our model on other types of hammer mills. In addition, other more mechanistic functions can also be exploited to broaden the applicability of the proposed model if they can take into account, in addition to material properties, particle size and process energy consumption. This will also enable the model to be more accurate beyond the limits of experimental conditions.

Declarations

Source of Funding

This research did not receive any grant from funding agencies in the public or not-for-profit sectors.

Competing Interests Statement

Authors have declared no competing interests.

Consent for Publication

The authors declare that they consented to the publication of this research.

Authors' Contributions

All the authors took part in literature review, analysis, and manuscript writing equally.

References

- [1] Ndjouenkeu Robert, Nzossie Eric Joël Fofiri, Kouebou Christiant, Njomaha Charles, Grembombo Adèle Irénée, et al. (2010). Le maïs et le niébé dans la sécurité alimentaire urbaine des savanes d'Afrique centrale. ISDA 2010, Juin 2010, Montpellier, France, 17 Pages.
- [2] Seutchueng Tchuenga Thierry Gaïtan, & Saha Frédéric (2017). Le maïs: une céréale à multiples usages au Cameroun sous la menace des contraintes climatiques et de ravageurs. Afrique Science, 13(6): 177–188.
- [3] Nzossié Éric Joël Fofiri, Ndamè Joseph-Pierre, Temple Ludovic, Dury Sandrine, & Ndjouenkeu Robert Kamdem Michel Simeu (2010). L'émergence du maïs dans la consommation alimentaire des ménages urbains au Nord-Cameroun. Économie rurale. doi: 10.4000/economierurale.2769.
- [4] Folefack D.P., & Abou S. (2016). Contribution à l'économie locale des micro-entreprises de transformation des céréales dans la ville de Maroua, Cameroun. Tropicultura, 34: 186–192.
- [5] Kengne Benjamin, Nzie Wolfgang, Tcheukam – Toko Dénis, & Ali Ahmed (2021a). Caractérisation des équipements de broyage des céréales de fabrication locale au Cameroun et évaluation de l'énergie consommée. Conférence Internationale LOREXP-2021, Chaines de Valeurs et Transformations Intégrales des Ressources Locales, Ngaoundéré, Cameroun, 20 au 23 Avril 2021.
- [6] Kwon Jihoe, Cho Heechan, Lee Daeyang, & Kim Rina (2014). Investigation of breakage characteristics of low rank coals in a laboratory swing hammer mill. Powder Technology, 256: 377–384. doi: <http://dx.doi.org/10.1016/j.powtec.2014.01.047>.
- [7] Thomas M., Hendriks W.H., & A.F.B. van der Poel (2018). Size distribution analysis of wheat, maize and soybeans and energy efficiency using different methods for coarse grinding. Anim. Feed Sci. Technol., 240: 11–21. doi: <https://doi.org/10.1016/j.anifeedsci.2018.03.010>.
- [8] Cotabarren Ivana, Fernández María Paz, Di Battista Agustina, & Piña Juliana (2020). Modeling of maize breakage in hammer mills of different scales through a population balance approach. Powder Technology, 375: 433–444. doi: <https://doi.org/10.1016/j.powtec.2020.08.016>.

[9] Rhodes M.J. (2008). *Introduction to Particle Technology*. 2nd Ed., Wiley & Sons, Chichester, England.

[10] Gil M., Luciano E., & Arauzo I. (2015). A Population balance model for biomass milling. *Powder Technology*, 276: 34–44. doi: <https://doi.org/10.1016/j.powtec.2015.01.060>.

[11] Gupta V.K. (2018). Understanding production of fines in batch ball milling for mill scale-up design using the population balance model. *Advanced Powder Technology*. doi: <https://doi.org/10.1016/j.apt.2018.05.010>.

[12] Gupta Ashok, & Yan Denis (2016). *Mineral Processing Design and Operations: An introduction* (Second Edition), Elsevier, 882 Pages, Chapter 11 - Mathematical Modelling of Comminution Processes, Pages 317–355.

[13] Gupta V.K. (2016). Determination of the specific breakage rate parameters using the top- size-fraction method: Preparation of the feed charge and design of experiments. *Advanced Powder Technology*, 27(4): 1710–1718. doi: <https://doi.org/10.1016/j.apt.2016.06.002>.

[14] Vukmirović D.M., Lević J.D., Fišteš A.Z., Čolović R.R., & Brlek T.I. (2016). Influence of grinding method and grinding intensity of corn on mill energy consumption and pellet quality. *Hem. Ind.*, 70: 67–72.

[15] Jindal V.K., & Austin L.G. (1976). The kinetics of hammer milling of maize, *Powder Technol.*, 14: 35–39. doi: [https://doi.org/10.1016/0032-5910\(76\)80005-8](https://doi.org/10.1016/0032-5910(76)80005-8).

[16] Austin L.G. (2004). A preliminary simulation model for fine grinding in high speed hammer mills. *Powder Technol.*, Pages 240–252. doi: <https://doi.org/10.1016/j.powtec.2004.04.017>.

[17] Nazari, M., Bilyera, N., Banfield, C.C. et al. (2023). Soil, climate, and variety impact on quantity and quality of maize root mucilage exudation. *Plant Soil*, 482: 25–38. doi: <https://doi.org/10.1007/s11104-022-05669-x>.

[18] Ajayi O.A., & Clarke B. (1997). High velocity impact of maize kernels, *J. Agric. Engineering Res.*, 67: 97–104. doi: <https://doi.org/10.1006/jaer.1997.0156>.

[19] El Shal M.S., Tawfik M.A., El Shal A.M., & Metwally K.A. (2010). Study the effect of some operational factors on hammer mill. *J. Agric. Eng. Res.*, 27: 54–74. doi: <https://doi.org/10.21608/mjae.2010.106853>.

[20] Saensukjaroenphon M. (2017). The effect of hammer mill screen hole diameter and hammer tip speed on particle size and flowability of ground corn. *Kansas Agric. Exp. Stn. Res. Reports*, 3: 1–7.

[21] Budăcan Ioan, Dumitru Pop & Ioan Drocaş (2013a). Specific energy consumption for reducing the size of maize grains using a hammer mill. *ACTA Technica Napocensis Series: Applied Mathematics and Mechanics*, 56(3): 479–484.

[22] Budăcan Ioan, Dumitru Pop & Ioan Drocaş (2013b). Size distribution of maize milled particles obtained by using a hammer mill. *ACTA Technica Napocensis Series: Applied Mathematics and Mechanics*, 56(4): 631–636.

[23] Lyu F., Van der Poel A.F.B., Hendriks W.H., & Thomas M. (2021). Particle size distribution of hammer-milled maize and soybean meal, its nutrient composition and in vitro digestion characteristics. *Animal Feed Science and Technology*, 281: 115095. doi: <https://doi.org/10.1016/j.anifeedsci.2021.115095>.

[24] Austin L.G., Jindal V.K., & Gotsis C. (1979). A model for continuous grinding in a laboratory hammer mill. *Powder Technol.*, 22: 199–204. doi: [https://doi.org/10.1016/0032-5910\(79\)80027-3](https://doi.org/10.1016/0032-5910(79)80027-3).

[25] Meloy T.P., & Williams M.C. (1992). Problems in population balance modelling of wet grinding. *Powder Technol.*, 71: 273–179.

[26] Tavares M. (2007). Breakage of single particles: quasi-static. *Handbook of Powder Technology*. doi: [https://doi.org/10.1016/S0167-3785\(07\)12004-2](https://doi.org/10.1016/S0167-3785(07)12004-2).

[27] Epstein B. (1948). Logarithmico-normal distribution in breakage of solids. *Ind. Chem.*, 40: 2289–2291.

[28] Scarlett B. (2002). Particle Populations-to balance or not to balance, that is the question. *Powder Technology*, 125: 1–4.

[29] Naimi Ladan Jafari (2008). Experiments and modeling of size reduction of Switchgrass in a laboratory rotary knife mill. Master of Applied Science, University of British Columbia, Canada, 103 Pages.

[30] Bertin D., Cotabarren I., Piña J., & Bucalá V. (2016). Population balance discretization for growth, attrition, aggregation, breakage and nucleation, *Comput. Chem. Eng.*, 84: 132–150. doi: <https://doi.org/10.1016/j.compchemeng.2015.08.011>.

[31] Bilgili, E., & Scarlett, B. (2005). Population balance modeling of non-linear effects in milling processes. *Powder Technology*, 153(1): 59–71. doi: <https://doi.org/10.1016/j.powtec.2005.02.005>.

[32] Reynolds G.K. (2010). Modelling of pharmaceutical granule size reduction in a conical screen mill. *Chem. Eng. J.*, 164: 383–392. doi: <https://doi.org/10.1016/j.cej.2010.03.041>.

[33] Vogel L., & Peukert W. (2005). From single particle impact behaviour to modelling of impact mills. *Chem. Eng. Sci.*, 60: 5164–5176. doi: <https://doi.org/10.1016/j.ces.2005.03.064>.

[34] Barrasso D., Oka S., Muliadi A, Litster J.D., Wassgren C., & Ramachandran R. (2013). Population balance model validation and prediction of CQAs for continuous milling processes: toward QbD in pharmaceutical drug product manufacturing. *J. Pharm Innov.*, 8: 147–162. doi: <https://doi.org/10.1007/s12247-013-9155-0>.

[35] Chimwani Ngonidzashe & Bwalya Murray M. (2021). Milling Studies in an Impact Crusher I: Kinetics Modelling Based on Population Balance Modelling. *Minerals*, 11(470):1-16. doi: <https://doi.org/10.3390/min11050470>.

[36] Reid K.J. (1965). Chemical engineering science, 20: 953–963.

[37] Austin L.G., Kliment R.R., & Luckie P.T. (1984). The Process Engineering of Size Reduction: Ball Milling. Society of Mining Engineers of the AIME, New York, Chapter 13, 102 Pages.

[38] Snow R.H., Allen T., Ennis B. J., & Litster J.D. (1997). Size reduction and size enlargement. In: R.H. Perry, D.W. Green (Eds.), *Perry's Chemical Engineers' Handbook*, McGraw-Hill.

[39] Chamayou Alain & Fages Jacques (2003). Broyage dans les industries agroalimentaires. Jean-Pierre Melcion et Jean-Luc Ilari. *Technologie des pulvérulents dans les IAA*, Lavoisier, Pages 375-406, Sciences et Techniques Agroalimentaires, 2-7430-0621-8.

[40] S. Nikolov (2004). Modelling and simulation of particle breakage in impact crushers. *Int. J. Miner. Process.*, 74: 219–225. doi: [10.1016/j.minpro.2004.07.031](https://doi.org/10.1016/j.minpro.2004.07.031).

[41] Petrakis, E., Stamboliadis, E., & Komnitsas, K. (2017). Identification of Optimal Mill Operating Parameters during Grinding of Quartz with the Use of Population Balance Modeling. *KONA Powder Journal*, 34: 213 – 223.

[42] Pandya J., & Spielman L. (1983). Floc breakage in agitated suspensions: effect of agitation rate. *Chem Eng Sci.*, 38(12): 1983–1992.

[43] Chaudhury Anwesha, Sen Maitraye, Barrasso Dana & Ramachandran Rohit (2016). Population Balance Models for Pharmaceutical Processes. In: Marianthi G. Ierapetritou and Rohit Ramachandran (eds.), *Process Simulation and Data Modeling in Solid Oral Drug Development and Manufacture, Methods in Pharmacology and Toxicology*. doi: https://doi10.1007/978-1-4939-2996-2_2.

[44] Austin L.G., & Luckie P.T. (1972). The estimation of non-normalized breakage distribution parameters from batch grinding tests. *Powder Technology*, 5(5): 267–271. doi: [https://doi:10.1016/0032-5910\(72\)80030-5](https://doi:10.1016/0032-5910(72)80030-5).

[45] Austin L.G., & Luckie P.T. (1971). The estimation of non-normalized breakage distribution parameters from batch grinding tests. *Powder Technol.*, 5: 267–271. doi: [https://doi.org/10.1016/0032-5910\(72\)80030-5](https://doi.org/10.1016/0032-5910(72)80030-5).

[46] Austin L.G., & Luckie P.T. (1972). Methods for determination of breakage distribution parameters. *Powder Technol.*, 5: 215–222. doi: [https://doi.org/10.1016/0032-5910\(72\)80022-6](https://doi.org/10.1016/0032-5910(72)80022-6).

[47] Berthiaux H., Varinot C., & Dodds J. (1996). Approximate calculation of breakage parameters from batch grinding tests. *Chemical Engineering Science*, 51(19): 4509–4516. doi: [https://doi:10.1016/0009-2509\(96\)00275-8](https://doi:10.1016/0009-2509(96)00275-8)

[48] Capece M., Bilgili E., & Dave R. (2011). Identification of the breakage rate and distribution parameters in a non-linear population balance model for batch milling. *Powder Technology*, 208(1): 195–204. doi: <https://doi:10.1016/j.powtec.2010.12.019>.

[49] Erasto Elias, Bashira A. Majaja, Said Ibrahim & Emmanuel G.R. Kizima (2014). *Tanzania Journal of Engineering and Technology*, 35(1): 34–45.

[50] Tosho A.S., Adeshina A.I., Salawu M., & Tope A.J. (2015). Prevalence of respiratory symptoms and lung function of flour mill workers in Ilorin, North Central Nigeria. *International Jour of Res and Review*, 2(3): 55–56.

[51] Iyogun K, Lateef S.A., & Ana G R.E.E. (2018). Lung function of grain millers exposed to grain dust and diesel exhaust in two food markets in Ibadan metropolis, Nigeria. *Safety and Health at Work*. doi: [10.1016/j.shaw.2018.01.002](https://doi:10.1016/j.shaw.2018.01.002).

[52] Kengne Benjamin, Ndibi Mbozo'o M.P., Samon Jean B., Nzie Wolfgang, Tcheukam – Toko Dénis, Ali Ahmed (2021b). Investigation on single-particle impact breakage functions of a « shaba » hybrids variety of maize kernel by drop-weight technique. *International Journal of Scientific and Research Publications*, 11(11). doi: [10.29322/IJSRP.11.11.2021.p11940](https://doi:10.29322/IJSRP.11.11.2021.p11940).

[53] Austin L.G. (1999). A discussion of equations for the analysis of batch grinding data. *Powder Technol.*, 106: 71–77. doi: [https://doi.org/10.1016/S0032-5910\(99\)00047-9](https://doi.org/10.1016/S0032-5910(99)00047-9).

[54] L.M. Tavares, R.M. de Cavalho, B. Bonfils & A.L.R. de Oliveira (2020). Back calculation of particle fracture energies using data from rotary breakage testing devices. *Minerals Engineering*, 149: 106263. doi: <https://doi.org/10.1016/j.mineng.2020.106263>.

[55] Klimpel R.R., & Austin L.G. (1970). Determination of Selection-for-Breakage Functions in the Batch Grinding Equation by Nonlinear Optimization. *Industrial & Engineering Chemistry Fundamentals*, 9(2): 230–237. doi: <https://doi:10.1021/i160034a007>.

[56] Kwon, J., & Cho, H. (2021). Investigation of Error Distribution in the Back-Calculation of Breakage Function Model Parameters via Nonlinear Programming. *Minerals*, 11: 425. doi: <https://doi.org/10.3390/min11040425>.

[57] R.H. Byrd, M.E. Hribar & J. Nocedal (1999). An interior point algorithm for large scale nonlinear programming. *SIAM J. Optim.*, 9: 877–900.

[58] FAO CXS 154–1985. 2.1, Codex Alimentarius.

[59] Mugabi, R., Eskridge, K.M., & Weller, C.L. (2017). Comparison of experimental designs used to study variables during hammer milling of corn bran. *American Society of Agricultural and Biological Engineers*, 60: 537–544. doi: <https://doi.org/10.13031/trans.11656>.

[60] Oka Y., & Majima H. (1970). A theory of size reduction involving fracture mechanics. *Canadian metallurgical Quarterly*, 9(2): 429–439. doi: <https://doi.org/10.1179/cmq.1970.9.2.429>.

[61] Fuerstenau D.W., Kapur P.C., & De A. (2003). Modeling breakage kinetics in various dry comminution systems. *KONA*, 21: 121–131.

[62] Chimwani, N., Glasser, D., Hildebrandt, D., Metzger, M.J., & Mulenga, F.K. (2013). Determination of the milling parameters of a platinum group minerals ore to optimize product size distribution for flotation purposes. *Miner. Eng.*, 43: 67–78.

[63] De Carvalho R.M., & Tavares L.M. (2013). Predicting the effect of operating and design variables on breakage rates using the mechanistic ball mill model. *Miner. Eng.*, 43–44: 91–101. doi: <https://doi.org/10.1016/j.mineng.2012.09.008>.